Interface polarization evolution during electroosmosis: an LSV-based in-operando investigation

Jian Zhou[1,2*], *Chaoyang* Xu[1,2,3], *Nicolò* Guarena[3], *Andrea* Dominijanni[3], and *Mario* Manassero[3]

[1] Coastal and Urban Geotechnical Engineering Research Center, Zhejiang University, Hangzhou, China
[2] Zhejiang Key Laboratory of the development and utilization of underground space, Hangzhou, China
[3] Department of Structural, Geotechnical and Building Engineering, Politecnico di Torino, Torino, Italy

Abstract. Interface energy consumption is well recognized as a limitation to the field-scale implementation of electroosmosis (EO). Although interface processes are regarded as crucial, conventional monitoring techniques remain restricted to the measurement of geotechnical parameters and fail to capture the time evolution of the electrode–soil interface during EO. To reveal the underlying mechanisms, linear sweep voltammetry (LSV) was employed to capture the polarization phenomena associated with the interface energy consumption. Specifically, a commonly used one-dimensional apparatus was integrated with a custom-designed LSV detection system, allowing continuous *in-operando* measurements during EO. The experimentally obtained polarization curves exhibit distinct regions, including an initial linear increase region, an intermediate segmented region, and a plateau region. Such time-dependent segmentation behaviour reflects different states of the electrode–soil interface, developing with the operating time. In particular, the increase in the interface energy consumption is attributed to a gradual transition in the interface conditions, shifting from a stable electrode–soil contact at the early stages to progressively clogged and transport-limited conditions at the later stages. Overall, this study demonstrates that LSV is a valuable tool for the effective monitoring of the electrode–soil interface evolution, and provides an engineering-oriented framework to interpret the interface energy consumption.

1 Introduction

In electroosmosis (EO), the energy consumption associated with the electric potential drop at the electrode–soil interface has been reported to constitute more than 30% of the total input energy. Moreover, this proportion increases progressively with treatment time and can exceed 80% during the advanced stages [1,2]. From a practical and economic perspective, such excessive energy consumption represents one of the primary factors limiting the large-scale engineering application of EO.

To tackle the issue of the interface energy consumption, various technical approaches have been proposed, including solution injection [3], enhancement by external magnetic fields [4], and bio-assisted EO [5], all of which have achieved partial reductions in the interface energy dissipation. However, the fundamental mechanisms governing the interface energy consumption remain insufficiently understood. At present, the experimental evidence on energy dissipation at the electrode–soil interface is predominantly interpreted according to Ohm's law, as exemplified by the models proposed by Zhuang and Wang [6], Xie et al. [7], Guo and Zhuang [8], and Sugiyama et al. [9]. Ohm's law is strictly applicable only to linear, steady-state, and chemically inert conductive systems, which are characterized by a linear relation between current and electric potential gradient [10]. In contrast, experimental observations during EO show that the electrode–soil interface undergoes continuous structural evolution over time. Processes such as surface deposition, film formation, and gas accumulation progressively modify the interface conditions, leading to non-linear and time-dependent current–potential responses [11,12]. These observations demonstrate that the electrode–soil interface cannot be adequately represented as a static Ohmic element. The complexity of the interface energy dissipation therefore arises not solely from electrical conduction, but also from the dynamic evolution of the interface itself. Changes in contact conditions of the interface, blockage of effective transport pathways, and partial detachment between the reaction zone and the surrounding pore network all contribute to the observed deviation from linear Ohmic behavior. As a result, a theoretical framework based on Ohm's law does not allow the individual contributions to the interface energy dissipation to be distinguished. This limitation is further compounded by the constraints of existing monitoring methods. Conventional evaluation approaches in electroosmotic ground improvement primarily rely on macroscopic indicators, such as gravimetric measurements of soil water content, direct shear tests for strength assessment, and visual inspection of soil cracking [13,14]. While these methods are effective for assessing the overall treatment

* Corresponding author: zjelim@zju.edu.cn

performance, they are not able to capture the progressive evolution of the electrode–soil interface, and therefore the processes responsible for the interface energy dissipation are not readily identified.

To address this gap, the present study adopts linear sweep voltammetry (LSV) as an *in-operando* monitoring technique to track the evolving response of the electrode–soil interface during EO. The primary objective is to elucidate how polarization behavior evolves over time as a manifestation of progressive changes in the interface structure. Based on a conventional one-dimensional electroosmotic setup, a customized LSV monitoring module was integrated to enable continuous electrode potential and current measurements throughout the electroosmotic process. In the experiments, copper electrodes embedded in high-salinity marine sludge were subjected to a constant direct-current electric potential difference, and polarization curves were recorded at predefined intervals. This study links the segmentation of the polarization response to different interface states, which developed over time during EO, and proposes an interpretation of the energy consumption at the interface in terms of its structural evolution, thereby providing a physically sound understanding of the investigated phenomenon for an optimal design of the electrodes.

2 Materials and methods

2.1 LSV-based measurement system

LSV allows the evolution of the electrode–soil interface in response to a variable electric potential to be investigated, yielding information that cannot be inferred from conventional geotechnical parameters. This measurement enables continuous monitoring of changes in polarization behavior that arise from the progressive evolution of the interface conditions during EO.

The system consists of a three-electrode configuration [15], in which the reference electrode provides a stable potential baseline, the working electrode represents the active electrode–soil interface, and the counter electrode completes the electrical circuit. During measurements, the potential of the working electrode is linearly swept from an initial to a final value, inducing a continuous evolution of the interface potential. In response to this imposed potential variation, the electric current adjusts continuously according to the instantaneous interface electrochemical and transport conditions. The resulting relationship between current and interfacial potential drop constitutes the polarization curve, which forms the basis for subsequent analysis. Variations in shape, segmentation, and temporal evolution reflect changes in interface connectivity, surface conditions, and transport pathways. These data provide a basis for tracking the progressive development of interface contact, interface clogging, and transport-limiting conditions, which together govern the evolution of the energy consumption at the interface.

Based on the working principles of LSV, a customized three-electrode system was developed. As shown in Fig. 2, a potential probe was positioned at a distance of 5 mm from the anode and served as the reference electrode to monitor electric potential drop at the anode's interface. This spacing was selected to minimize disturbance to the anode–sludge interface while maintaining measurement accuracy [10]. Because of the important role of the anode in EO [11], the present study focuses primarily on anodic processes. The probe was fabricated from copper following established practice reported in previous studies [12]. A HSPY 120 02 direct current power supply was used for real-time voltage regulation, enabling accurate control over the applied electric potential difference and scan rate. Electrode potential and current signals were recorded at a data acquisition rate of 8 Hz using a DW 81 C digital multimeter.

2.2 Tested materials

The sludge tested in this study was sampled in the proximity of a seawall located in Taizhou City, Zhejiang Province, China. The basic physical properties of the undisturbed sludge are summarized in Table 1.

Table 1. Basic physical properties of the tested sludge.

Properties	Value
Specific gravity, G_s	2.74
Plastic limit (%)	23
Liquid limit (%)	48
Water content (%)	61
pH	7.4
Electrical conductivity (S/m)	0.36

Prior to testing, soil samples were prepared as follows. The soil was oven-dried at 105 °C, pulverized, and subsequently sieved through a 2 mm mesh to obtain a uniform fine-grained material. The powdered soil was mixed with distilled water up to a moisture content of 85%, which falls within the typical testing range of 80–100% [4,13]. The prepared mixture was placed in the testing cell and gently vibrated for one minute at one-third filling increments to remove entrapped air. After the cell was fully filled, it was allowed to stand for 24 hours to permit residual air to escape.

2.3 Laboratory apparatus

Fig. 1 illustrates the setup of the experimental apparatus. The testing cell was fabricated from acrylic with a thickness of 1 cm. The electroosmotic cell measured 20 cm in length, 10 cm in width, and 10 cm in depth. Electrode plates were installed on both sides of the cell, and the cathode was perforated to facilitate drainage. Geotextile filters were placed behind the cathode to prevent soil particles from being carried away by the fluid flow.

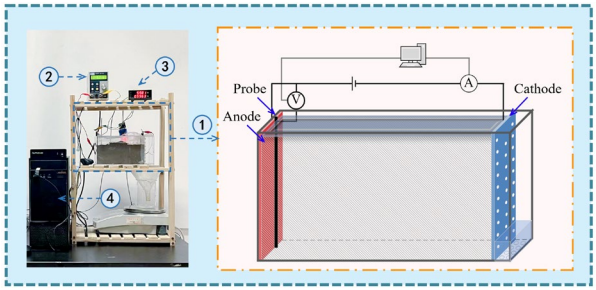

Fig. 1. Laboratory apparatus for EO tests. (1): testing cell; (2): DC power supply; (3): digital multimeter; (4): computer and data acquisition software.

2.4 Test methods

Copper was selected as the electrode material in this study, as copper is a commonly used electrode material in EO [11,13]. All the tests were conducted under an imposed electric potential difference of 30 V, which is commonplace in laboratory studies [16,17]. The scan rate was set to 0.1 $V \cdot s^{-1}$, according to previous recommendations [18,19]. This scan rate was selected to shorten the scanning duration and enable timely capture of the evolving polarization at the electrode–sludge interface, while simultaneously minimizing the volumetric strain of the sludge during testing and reducing interference with non-electrochemical factors. The electric potential difference was varied in the 0 to 30 V range to encompass the electrochemical response under typical electroosmotic operating conditions. Accordingly, this finite potential sweep was intended to capture the interface evolution during EO, rather than to serve as a traditional small-perturbation dielectric using a smaller excitation amplitude. To capture the transitional evolution of the electrode–sludge interface during EO, the present study focused on an operating period of 5 hours. During this period, five LSV scans were performed, with one scan conducted every hour, and each scan lasting 5 minutes. This one-hour measurement interval was selected to ensure sufficient temporal resolution, so as to capture the time-dependent evolution of the interface electrochemical properties while minimizing disturbance.

3 Results

3.1 Polarization curves

Fig. 2 presents the polarization curves of the copper electrode measured by LSV. For ease of comparison, all measurements are plotted using the same scale for the current and potential axes. As EO progresses, the polarization response exhibits a clear time-dependent evolution, demonstrating that the electrode–soil interface changes its electrochemical properties during operation. Notably, the polarization curves exhibit relatively regular shapes with clear transitions between different regions. Such polarization behavior is commonly observed in studies of corroding metal electrodes, which often exhibit multiple inflection points and distinct regions associated with different electrochemical mechanisms. Sugiyama et al. [9] reported polarization curves for iron, aluminum, and stainless steel electrodes that exhibit distinguishable regional transitions in EO. Compared with the present results, their polarization responses display more pronounced local fluctuations. By contrast, a slower scanning rate was adopted in the present study, leading to a more quasi-steady response and smoother polarization curves. In the present work, copper electrodes were employed, for which multi-segment polarization behavior with clear inflection points has been well documented in electrolyte solutions, such as NaCl, as reported by Alfantazi et al. [20]. However, compared with those studies conducted over a wider potential range, the voltage window adopted herein is relatively limited and the response is strongly influenced by the high-resistance soil matrix. Consequently, the observed polarization curves appear less complex.

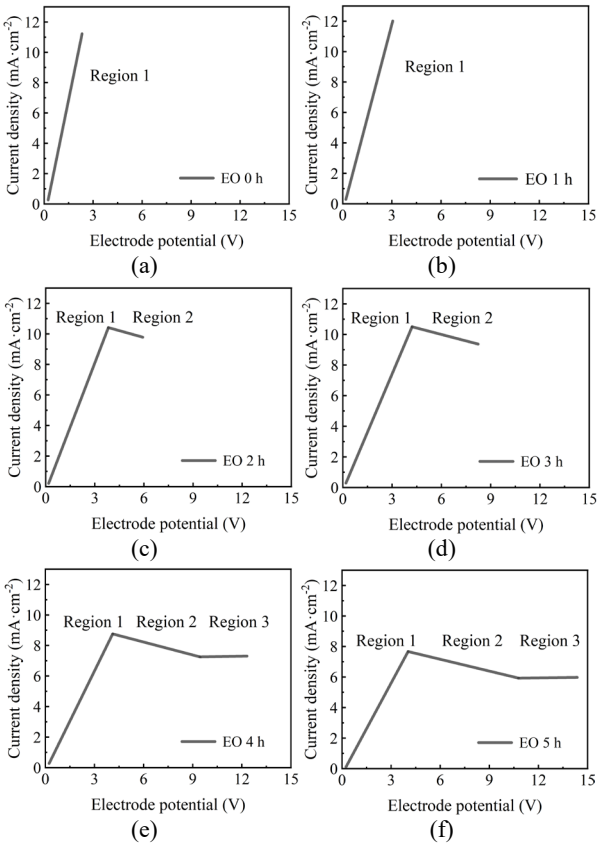

Fig. 2. LSV-derived polarization curves of the copper electrode at EO times from 0 to 5 h (a–f).

During the first two hours, the polarization curves display an approximately linear current–potential relation, which is consistent with the electrode behavior that is expected at the early stages of EO, as reported by Zheng et al. [21]. After approximately three hours, the curves deviate from the initial linearity and exhibit segmented linear behavior, which consists of two linear regions. At the fourth hour, a more pronounced multi-segment response is observed, accompanied by the evidence of a plateau region. Similar evolution patterns have been widely reported for copper, copper alloys, stainless steel, and other metals under sustained electrical loading [20,22]. For example, Alfantazi et al. [20] investigated the polarization behavior of pure copper and Cu-based alloys (Cu–Ni, Cu–Zn, and Cu–

Al) in chloride media and observed pronounced multi-segment polarization responses at the anode, associated with progressive surface film formation, degradation, and product accumulation. Therefore, these progressive changes in the anode polarization with operating time demonstrate that the electrode–soil interface undergoes continuous structural evolution.

3.2 Decomposition of the interface potential

If the electroosmotic cell is modelled as a series circuit and the system is assumed to be at steady state, the current density is the same at any location in the tested sludge. Accordingly, the electrode potential is directly related to the energy consumption at the anode [4]. This provides a quantitative basis for examining how the interface energy dissipation evolves during operation.

To facilitate the analysis, the electrode potential is partitioned according to the regions identified in the polarization curves. Specifically, the potential contributions associated with the initial linear region, the segmented linear region, and the plateau region are denoted as Region 1, Region 2, and Region 3, respectively. These regions correspond to different states of the electrode–soil interface that develop as EO proceeds.

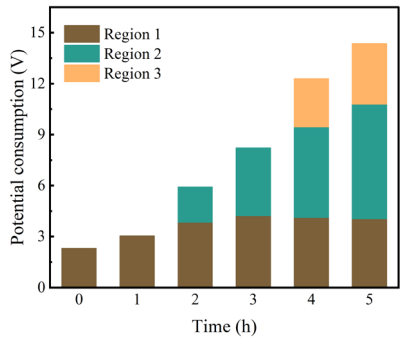

Fig. 3. Evolution of the electrode potential over time.

Fig. 3 illustrates the temporal evolution of the electrode potential and the associated contributions. The contribution of Region 1 exhibits relatively limited variation, increasing from 2.321 V to 3.827 V during the first two hours and stabilizing thereafter at approximately 4 V. In contrast, the contribution of Region 2 builds up after two hours from the beginning of the test, and increases rapidly from 2.103 V to 6.748 V at the end of the test. A similar monotonic increase is observed for the contribution of Region 3 after its onset, increasing from 2.870 V to 3.591 V.

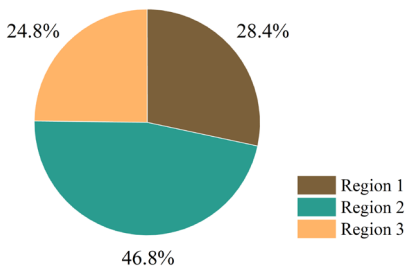

Fig. 4. Contributions to the electrode potential at the end.

As shown in Fig. 4, a detailed partitioning of the electrode potential after five hours from the beginning of EO shows that the contributions of Region 2 and Region 3 together account for 71.6% of the total potential drop at the anode's interface. This result demonstrates that the significant increase in the interface energy consumption during the later testing period is primarily associated with the progressive growth of these two contributions, whereas the contribution of Region 1 remains relatively stable for the whole testing duration. During the early period of operation, the energy dissipation at the anode's interface is therefore dominated by the contribution of Region 1, which accounts for nearly the entire interface potential drop, as shown in Fig. 3.

4 Discussion

Based on the time evolution of the polarization response, the interface energy consumption process can be subdivided into three consecutive stages, each corresponding to a different state of the electrode–soil interface governing the energy dissipation. The following subsections are devoted to interpreting the contribution of each dissipation mechanism, from the perspective of the time evolution of the interface conditions.

4.1 Contact-dominated interface regime

In the initial stage, the polarization curves exhibit an approximately linear relation between current and electrode potential. This behavior demonstrates that the electrode–soil interface remains relatively uniform and stable, being the energy consumption primarily associated with the contact conditions between the electrode surface and the surrounding soil. At this stage, the dominant interface processes include electrode–soil wetting, initial electrolyte redistribution, and the formation of continuous conductive pathways across the interface. Previous studies have reported that, during the early stage of EO, the interface resistance remains nearly constant over a wide current range, reflecting structurally stable interface conditions.

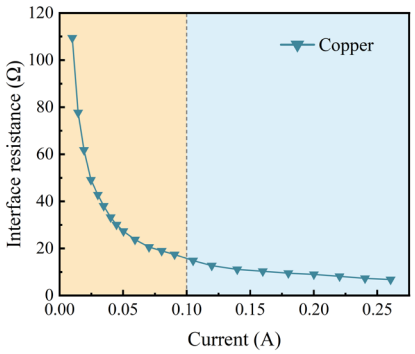

Fig. 5. Interface resistance of copper electrodes as a function of current (Guo et al. [8]).

Fig. 5 shows relevant measurements reported by Guo et al. [8], where the interface resistance of copper electrodes remains approximately constant at about 10 Ω over most of the current range, except at very low

currents below 0.1 A. Moreover, as the current increases, fluctuations in the interface resistance become progressively smaller, as a result of the enhanced interface stability.

These observations suggest that, during the early stage of EO, energy consumption is mainly associated with the electrical continuity across a well-connected electrode–soil interface, without any significant structural obstruction or charge-transfer limitation.

4.2 Clogging-affected interface regime

Subsequently, the polarization curves show a transition from a mono-linear to a bi-linear relation, reflecting a change in the state of the electrode–soil interface. In soils with relatively high sodium chloride concentrations, copper electrodes are prone to surface transformations such as oxide formation, particulate deposition, and interface cementation, as widely reported in previous laboratory studies [11,13]. The accumulation of these reaction products on the electrode surface alters the interface morphology, reduces the area that is effectively involved in the transport of electric current, and introduces additional constraints to the charge and mass transfer across the interface. Alfantazi et al. [20] reported that such surface transformations are commonly accompanied by inflection points and segmentation of the polarization curves, which are attributed to transitions between different interface conditions. Consistently with these findings, a clear inflection point separating the initial stage and the subsequent stage is observed in this study (Fig. 2). The observed inflection is interpreted as the onset of interface clogging, during which the energy consumption increases due to the obstruction associated with the formation of surface deposits. Accordingly, the increased energy demand in this second stage of EO is attributed to the structural degradation of the electrode–soil interface.

4.3 Crack-induced detachment interface regime

In the later stages, a plateau region builds up in the polarization curves, as a result of remarkable changes in the interface conditions. In this study, a noticeable detachment of the electrode from the surrounding sludge was observed from the fourth hour onward, which is consistent with previous experimental observations for prolonged EO operation [11,13]. As the reaction products accumulate at the electrode's surface, spatial separation occurs at the electrode–soil interface due to the formation of cracks, causing portions of the electrode surface to become isolated from the surrounding pore space and thereby hindering the charge transfer through the interface. Consequently, the connectivity between the electrode surface and the soil pore network weakens, leading to partial detachment of the interface reaction zone. Under such conditions, additional energy input is required to sustain the processes underlying the charge transfer at the interface, while the overall current density exhibits negligibly small changes, giving rise to a pronounced mismatch between energy input and transport efficiency. Based on visual observations during the experiments and their consistency with previous evidence, this mismatch is interpreted as the effect of a progressive loss of contact between the electrode surface and the pore fluid, which in turn is reflected in the plateau region of the polarization curves. A time-resolved correlation between energy efficiency and crack propagation was not quantified in the present study, and such quantitative interpretation is identified as an important direction for future research.

Based on the current observations, the expansion of Regions 2 and 3 is attributed to progressive interfacial degradation. However, due to the finite spacing between the potential probe electrodes, the measured response inevitably includes contributions not only from the interface itself but also from the adjacent sludge domain, including possible electrophoretic effects. Although such effects are generally considered to be limited, as the mobility of charged species is strongly constrained by the pore structure and solid–liquid interactions, and the solid particles themselves are difficult to transport through the restricted pore space [4], their specific contributions have not yet been clarified. Future research will therefore employ a multidisciplinary approach to elucidate the coupled mechanisms involved.

5 Conclusions

In this study, an *in-operando* monitoring approach was adopted to investigate the evolving response of copper electrode–soil interfaces during EO, with the aim to advance the understanding of the mechanisms underlying the energy consumption at the electrode interfaces. The main conclusions are summarized as follows:

(1) An interface monitoring approach applicable to EO processes was proposed and validated. This approach overcomes the limitations of conventional monitoring methods that rely solely on macroscopic geotechnical parameters and are unable to capture the evolution of the interface conditions.

(2) The segmentation of the polarization curves during EO and their time evolution were shown and discussed. The experimentally obtained polarization curves exhibit three distinct regions, including an initial linear increase region, an intermediate segmented region, and a plateau region. These regions correspond to different states of the electrode–soil interface, which develop over the operating time.

(3) From the perspective of the interface structural properties, the increase in the interface energy consumption is attributed to a gradual change in the interface conditions. Specifically, the interface shifts from a stable electrode–soil contact at the early stages to progressively blocked and transport-limited interface states at the later stages.

Future work will focus on clarifying the time evolution of the interface conditions. The present study monitored the EO processes primarily within the first five hours of operation, and additional interface evolution patterns may build up during a longer EO

treatment. The experimentally observed polarization responses should also be interpreted through physically sound theoretical models to better describe the change in time of the interface energy consumption during EO.

The study presented in this article was substantially supported by the National Natural Science Foundation of China (Grant Numbers 52478366, 52378378, 52078455, 51708507), Zhejiang Key Laboratory of the development and utilization of underground space (Grant Numbers 2025E10118), Zhejiang Province Water Conservancy Engineering Science and Technology Research Project (Grant Number RA+202303).

References

1. E. Mohamedelhassan, J. Q. Shang, Effects of electrode materials and current intermittence in electro-osmosis. Proceedings of the Institution of Civil Engineers - Ground Improvement **5**, 3 (2001). https://doi.org/10.1680/grim.2001.5.1.3
2. K. Zhang, L. Zheng, T. Zhao, X.Xie, Experimental study of arrangement type on the reinforcement effect of electric geotextile-encased stone columns in soft soil. Journal of Ground Improvement **5**, 105 (2023).
3. C. Y. Ou, S. C. Chien, H. H. Chang, Soil improvement using electroosmosis with the injection of chemical solutions: field tests. Can. Geotech. J. **46**, 727 (2009). https://doi.org/10.1139/T09-012
4. C. Xu, J. Zhou, Y. Jiang, Y. Tao, R. Chen, Experimental study on improved method of electroosmosis combined with magnetic field. Acta Geotech. **20**, 3439 (2025). https://doi.org/10.1007/s11440-025-02575-1
5. G. Guan, Y. Shen, J. Feng, K. Fan, Behavior of drainage and chemical consolidation during electroosmosis in soil: A review. Drying Technology **43**, 2020 (2025). https://doi.org/10.1080/07373937.2025.2562256
6. Y. F. Zhuang, Z. Wang, Interface Electric Resistance of Electroosmotic Consolidation. J Geotech Geoenviron **133**, 1617 (2007). https://doi.org/10.1061/(asce)1090-0241(2007)133:12(1617)
7. X. Xie, Z. Li, L. Zheng, J. Li, Y. Liu, Experimental study on influencing factors of contact resistance on electroosmotic consolidation. Journal of Central South University (Science and Technology) **49**, 655 (2018).
8. K. S. Guo,Y. F. Zhuang, Measurement methodology and characteristics of interfacial resistance in electro-osmosis. Geosynthetics International **30**, 460 (2023). https://doi.org/10.1680/jgein.22.00156
9. Y. Sugiyama, N. Hashimoto, C. Couture, D. Takano, Electrochemical perspective on the applicability of electroosmosis for clay consolidation. J Appl Electrochem **54**, 1057 (2024). https://doi.org/10.1007/s10800-023-02018-3
10. C. Xu, J Zhou., Y. Jiang, Y. Tao, X. Liu, Experimental Analysis of Potential Drop at Soil Electrode Interface of Electroosmosis Based on Linear Sweep Voltammetry. Journal of Shanghai Jiaotong University **1** (2025). https://doi.org/10.16183/j.cnki.jsjtu.2025.151
11. Z. Xue, X. Tang, Q. Yang, Y. Wan, G. Yang, Comparison of Electro-Osmosis Experiments on Marine Sludge with Different Electrode Materials. Dry Technol **33**, 986 (2015). https://doi.org/10.1080/07373937.2015.1011274
12. C. Xu, J. Zhou, W. Zhou, Y. Jiang, Z. Zhu, J. Yu, Experimental study on enhancing efficiency of electroosmotic reinforcement with magnetic field. Chinese Journal of Geotechnical Engineering **46**, 77 (2024). https://doi.org/10.11779/CJGE2024S20003
13. J. Zhou, Y. L. Tao, C. J. Xu, X. N. Gong, P. C. Hu, Electro-osmotic strengthening of silts based on selected electrode materials. Soils Found **55**, 1171 (2015). https://doi.org/10.1016/j.sandf.2015.09.017
14. C. Feng, S. Ge, L. Zheng, X. Xie, Introduction to new technologies for soft soil foundation treatment based on electro-osmosis method. Journal of Ground Improvement **7**, 603 (2025).
15. L. Wu, Z. Pan, S. Yuan, X. Shi, Y. Liu, F. Liu, X. Yan, L. An, A dual-layer flow field design capable of enhancing bubble self-pumping and its application in water electrolyzer. Chemical Engineering Journal **488**, 151000 (2024). https://doi.org/10.1016/j.cej.2024.151000
16. Y. Jiang, J. Zhou, Q. Gan, Y. Ma, W. Shi, Experimental study on the effect of reversal voltage to electro-osmosis using polarity reversal method. Journal of Ground Improvement **4**, 37 (2022).
17. Y. Tao, J. Zhu, J. Zhou, X. Gong, Z. Yu, K. Li, Experimental study on electro-osmotic conductivity of Hangzhou sludge. Acta Geotech. **19**, 5337 (2024). https://doi.org/10.1007/s11440-024-02228-9
18. Z. Wang, Y. Li, C. Zhang, J. Wu, K. Cui, Q. Li, Degradation of AO7 through RGO/TiO2 nanotube arrays photoanode in UV/electrical coupling system: performance and mechanism analysis. Optical Materials **149**, 115030 (2024). https://doi.org/10.1016/j.optmat.2024.115030
19. O. S. Ivanova, F. P. Zamborini, Electrochemical Size Discrimination of Gold Nanoparticles Attached to Glass/Indium−Tin-Oxide Electrodes by Oxidation in Bromide-Containing Electrolyte. Anal. Chem. **82**, 5844 (2010). https://doi.org/10.1021/ac101021q
20. A. M. Alfantazi, T. M. Ahmed, D. Tromans, Corrosion behavior of copper alloys in chloride media. Materials & Design **30**, 2425 (2009). https://doi.org/10.1016/j.matdes.2008.10.015
21. Q. Zheng, A. Deng, M. Jaksa, Modeling instantaneous interfacial voltage drop in electroosmosis. Electrochimica Acta **548**, 147987 (2026). https://doi.org/10.1016/j.electacta.2025.147987
22. E. E. Oguzie, J. Li, Y. Liu, D. Chen, Y. Li, K. Yang, F. Wang, The effect of Cu addition on the electrochemical corrosion and passivation behavior of stainless steels. Electrochimica Acta **55**, 5028 (2010). https://doi.org/10.1016/j.electacta.2010.04.015